Author Manuscript

Author Manuscript

Author Manuscript

Author Manuscript

HHS Public Access

Author manuscript

ACS Nano. Author manuscript; available in PMC 2017 June 28.

Published in final edited form as:

ACS Nano. 2016 June 28; 10(6): 6008–6019. doi:10.1021/acsnano.6b01560.

Toxicological Profiling of Highly-Purified Metallic and Semiconducting Single-Walled Carbon Nanotubes in the Rodent Lung and *E. coli*

Xiang Wang[†,‡], **Nikhita D. Mansukhani**[ς], **Linda M. Guiney**[ς], **Jae-Hyeok Lee**[ς], **Ruibin Li**[†], **Bingbing Sun**[†], **Yu-Pei Liao**[†], **Chong Hyun Chang**[‡], **Zhaoxia Ji**[‡], **Tian Xia**[†,‡], **Mark C. Hersam**[ς], and **André E. Nel**[†,‡,*]

[†]Division of NanoMedicine, Department of Medicine, University of California, Los Angeles, CA 90095, United States

[‡]California NanoSystems Institute, University of California, Los Angeles, CA 90095, United States

[ς]Departments of Materials Science and Engineering, Chemistry, and Medicine, Northwestern University, Evanston, Illinois 60208, United States

Abstract

The electronic properties of single-walled carbon nanotubes (SWCNTs) are potentially useful for electronics, optics, and sensing applications. Depending on the chirality and diameter, individual SWCNTs can be classified as semiconducting (S-SWCNT) or metallic (M-SWCNT). From a biological perspective, the hazard profiling of purified metallic *versus* semiconducting SWCNTs has only been pursued in bacteria, with the conclusion that aggregated M-SWCNTs are more damaging to bacterial membranes than S-SWCNTs. However, no comparative studies have been performed in a mammalian system, where most toxicity studies have been undertaken using relatively crude SWCNTs that include a M:S mix at 1:2 ratio. In order to compare the toxicological impact of SWCNTs sorted to enrich them for each of the chirality on pulmonary cells and the intact lung, we used density gradient ultracentrifugation and extensive rinsing to prepare S- and M-SWCNTs that are >98% purified. *In vitro* screening showed that both tube variants trigger similar amounts of interleukin 1β (IL-1β) and transforming growth factor (TGF-β1) production in THP-1 and BEAS-2B cells, without cytotoxicity. Oropharyngeal aspiration confirmed that both SWCNT variants induce comparable fibrotic effects in the lung and abundance of IL-1β and TGF-β1 release in the bronchoalveolar lavage fluid. There was also no change in the morphology, membrane integrity, and viability of *E. coli*, in contradistinction to the previously published effects of aggregated tubes on the bacterial membrane. Collectively, these data indicate that the electronic properties and chirality do not independently impact SWCNT toxicological impact in the lung, which is of significance to the safety assessment and incremental use of purified tubes by industry.

[*]Corresponding Author: André E. Nel, M.D./Ph.D., Department of Medicine, Division of NanoMedicine, UCLA School of Medicine, 52-175 CHS, 10833 Le Conte Ave, Los Angeles, CA 90095-1680. Tel: (310) 825-6620, Fax: (310) 206-8107, anel@mednet.ucla.edu.

Supporting Information Available: Data on cell association, cellular ROS generation, *in vivo* differential cell counts, H&E staining and TEM images of E coli are available free of charge *via* the Internet at http://pubs.acs.org.

Author Manuscript Author Manuscript Author Manuscript Author Manuscript

Graphical Abstract

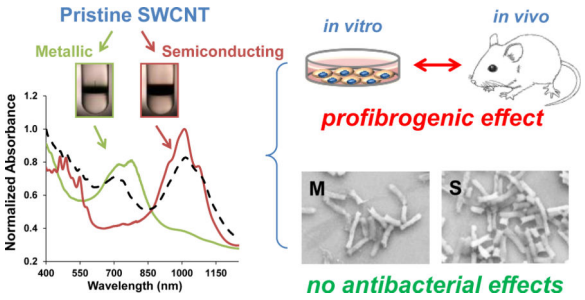

Keywords

SWCNT; electronic property; semiconductor; metallic; lung toxicity; bacteria

Purified single-walled carbon nanotubes (SWCNTs) have superlative electrical properties for promising applications in electronics.[1] However, SWCNTs, as synthesized, have a wide range of diameters and chiral angles which leads to a polydisperse sample of discrete properties. Depending on these chiral angles and diameters, SWCNTs may be semiconducting (S-SWCNT) or metallic (M-SWCNT) in nature.[2–4] In general, as-synthesized SWCNTs are comprised of S-SWCNTs and M-SWCNTs in an approximately 2:1 ratio. S-SWCNTs exhibit high current density, high electron/hole mobility, and display a direct band gap that is inversely proportional to diameter.[2–4] This allows their use as conductive channels in field-effect transistors, allowing high on/off ratios for logic device applications.[2] In contrast, due to their metallic conductance properties, M-SWCNTs can function as effective nanoscale sensor electrodes that can be used in applications such as transparent conducting films or interconnects for integrated circuits.[2–4] However, the realization of these applications is dependent on the production of high purity SWCNTs that can be sorted by diameter and chiral angle in order to exploit their exceptional electronic properties.

The chirality of SWCNTs could also be significant from a biological perspective, including their hazard potential. Most toxicological studies have focused on polydisperse SWCNT formulations, which exhibit pulmonary hazard potential based on material attributes such as the method of production, metal and carbon impurities, tube length, reactive carbon surfaces, surface defects and functionalities.[5–23] Experimental studies on SWCNTs in rodents have also shown that bolus installation as well as aerosolized inhalation exposures can induce acute lung injury as well as subchronic granulomatous inflammation and fibrosis in the lung.[6–20,22–24] This includes our own demonstration that crude, as-purchased (AP) or purified (*e.g.*, eliminating metal contamination) SWCNTs can trigger pro-fibrogenic effects in the lung, regardless of the synthesis method.[16,18] The literature also documents that SWCNT properties such as length, diameter, impurity, carbon-based surface reactivity or surface functionalization can impact the severity of lung injury. In contrast, tube dispersal and passivation by coating with a biocompatible triblock copolymer (Pluronic F108) showed a dramatic reduction in hazard potential in the lung.[13,15] While often talked about as a possible contributing factor, there is a paucity of data regarding the biological impact of

Author Manuscript Author Manuscript Author Manuscript Author Manuscript

chirality because of the challenges to obtain highly purified metallic and semiconducting materials for biological experimentation. The most detailed study of the role of SWCNT electronic properties in *Escherichia coli (E. coli)* demonstrated that metallic tubes have an exaggerated effect on bacterial viability and membrane permeability based on the pro-oxidative effects compared to semiconductor SWCNTs.[25] Moreover, the antibacterial effects was dependent on direct binding of aggregated, metallic SWCNTs to the bacterial membrane.[25]

Density gradient ultracentrifugation (DGU) allows fractionation of polydisperse SWCNTs into highly purified M- and S-SWCNTs.[2,5,26] This method has allowed us to gather a representative library of SWCNTs, including S-SWCNTs, M-SWCNTs, unsorted (P2) SWCNTs or a remixed sample containing purified S-SWCNTs and M-SWCNTs in a 2:1 ratio. These materials are unique for the high purity levels (98.5 % S-SWCNT and 98.8 % M-SWCNT) as well as state of dispersion in aqueous biological media. We present a comprehensive analysis of the pulmonary hazard potential of these materials *in vitro* and *in vivo*, which indicate that in spite of differences in the ability to induce ROS and oxidative stress, the toxicological outcome in the lung is equivalent for M- and S-SWCNTs. We also performed a comparative analysis in *E. coli*, which demonstrated a lack of anti-bacterial effects of the well-dispersed SWCNT variants. These data are of considerable importance for considering whether to use chirality to categorize SWCNTs for regulatory purposes, particularly since the market access of purified SWCNTs is expected to increase.

RESULTS

Fractionation, purification and characterization of semiconducting (S-) and metallic (M-) SWCNTs

SWCNTs were sorted into metallic and semiconducting variants using density gradient ultracentrifugation of a batch of arc-discharge SWCNTs (designated P2) according to the scheme depicted in Figure 1A. Following the removal of detergent by ethanol precipitation and extensive rinsing in deionized (DI) water, the purified M-SWCNT and S-SWCNT dispersions exhibited purities of >98.8% and >98.5%, respectively (Figure 1B). Figure 1B also shows the absorbance spectrum of the unsorted tubes by optical absorbance spectroscopy. The Arc discharge method employs nickel and yttrium as catalysts. ICP-MS was used to determine the amount of residual catalyst in each sample (Table S1). Briefly, all three (P2-, M- and S-) SWCNT preparations show a Ni content of ∼ 2.40 wt % and an Yi content of ∼ 0.43 wt %. Measurement of the size of the sorted SWCNTs by atomic force microscopy (AFM) demonstrated that the semiconducting tubes had an average length of 633 nm and an average diameter of 1.29 nm; the corresponding values for metallic tubes were 634 nm and 1.24 nm, respectively (Figure 1C and 1D). The AFM images also demonstrate excellent dispersion of individual tubes, including narrow length and diameter distributions (Figure 1C and 1D). The corresponding hydrodynamic diameters of the sorted tubes in DI water, complete RPMI medium (containing 10 % FCS), and BEGM (containing 0.6 mg/mL bovine serum albumin and 0.01 mg/mL DPPC), as determined by high-throughput dynamic light scattering (HT-DLS, Dynapro Plate Reader, Wyatt Technology), are shown in Table 1. Following dispersion in DI water, the hydrodynamic sizes of S- and

Author Manuscript Author Manuscript Author Manuscript Author Manuscript

M-SWCNTs were 807 and 1192 nm, respectively. Similar trends were seen in BEGM and RPMI media (Table 1). There was slightly better dispersion of the unsorted (P2) arc-discharge SWCNTs in both media (Table 1). The zeta potentials of the tubes ranged from −4.3 to −8.8 mV in cell culture media and −12.9 to −34.3 mV in water (Table 1).

S- and M-SWCNTs do not differ in cytotoxic potential and pro-inflammatory effects *in vitro*

The cytotoxicity and pro-inflammatory effects of sorted SWCNTs were studied in THP-1 and BEAS-2B cell lines. The myeloid cell line (THP-1) was chosen for its ability to differentiate into macrophage-like cells that exhibit NLRP3 inflammasome assembly in response to high aspect ratio (HAR) materials (such as CNTs), while BEAS-2B is an immortalized human bronchial epithelial cell line that responds to CNTs with TGF-β1 production.[15,27–29] Both cell types represent portal-of-entry cells that come into early contact with nanomaterials in the lung. An MTS assay was used to demonstrate that purified S- and M-SWCNTs, as well as P2- or remixed SWCNTs, failed to affect cell viability (Figure 2A, B). In contrast, there was a significant decrease in cell viability in response to nano-ZnO, used as a positive control. A similar analysis using an assay that measures cellular ATP content showed that there was no effect on cellular viability (Figure S2A and B). We also did not observe an effect on cellular membrane lysis using an LDH assay (not shown). In addition, the use of an IL-1β assay to demonstrate the impact of the SWCNTs on NLRP3 inflammasome assembly showed a dose-dependent increase in cytokine production for all tube variants in THP-1 cells (Figure 3A and S2C). The increased IL-1β production could be detected at 24 hr but not at 3 and 6 hr (Figure S2E). Monosodium urate (MSU) was used as a positive control that induced the strongest effect. Importantly, there was no significant difference in the pro-inflammatory effects of S- *versus* M-SWCNTs. While the assessment of TGF-β1 production in BEAS-2B yielded less vigorous stimulation indices (Figure 3B and S2D), it was confirmed that S-SWCNTs do not differ from M-SWCNTs (Figure 3B and S2D). IL-1β and TGF-β1 play an important and synergistic role in the generation of epithelial-mesenchymal transition (EMT) and the subsequent cascade that culminates in pulmonary fibrosis in response to HAR materials, such as CNTs.

The pro-inflammatory and pro-fibrogenic effects of SWCNTs require uptake and lysosomal processing in THP-1 and BEAS-2B cells, which is dependent on the colloidal stability and the sedimentation of aggregated *versus* suspended tubes in biological media.[11,17,30] Therefore, we compared the suspension stability index of the different tube variants in the tissue culture media that are used for THP-1 cells (*i.e.*, RPMI 1640) and BEAS-2B cells (*i.e.*, BEGM), respectively. This demonstrated that, except for some degree of sedimentation in the first five hours, all the tube types remained well suspended over a 24 hr observation period (Figure 4A and B). S-SWCNTs did not differ from M-SWCNTs in their colloidal stability. It was further demonstrated by flow cytometry (side scatter analysis) that there was no difference in the relative abundance of cellular association of the different tube types (Figure S3), indicating that there were no significant variances in the cellular exposure levels for S- and M-SWCNTs. This is in agreement with the IL-1β data (Figure 3A).

Author Manuscript Author Manuscript Author Manuscript Author Manuscript

Another important SWCNT characteristic to consider in the cellular response outcome is the electron transfer capabilities of metallic *versus* semiconducting SWCNTs, which could lead to the generation of reactive oxygen species (ROS) and oxidative stress, as shown in bacterial studies.[25] An abiotic assay to compare ROS production, using the fluorescent dye, 2', 7'-dichlorofluorescein (DCF), was performed. Performance of spectroscopy at 528 nm demonstrated a dose-dependent increase in fluorescence intensity, with M-SWCNTs inducing more ROS generation than S-SWCNTs (Figure 4C and D). Co_3O_4, a semiconductor metal oxide, was used as a positive control.[31] Oxidant injury can also be determined by assessing glutathione (GSH) conversion to GSSG, as determined by luminescence-based GSH-Glo assay. Use of this assay under abiotic conditions confirmed that M-SWCNTs lead to more GSH depletion than S-SWCNTs (Figure 4E). No significant differences were observed between M-SWCNTs, P2-SWCNTs or remixed tubes in this assay (Figure 4E). When using the GSH-Glo assay to determine the induction of oxidative stress in THP-1 and BEAS-2B cells, both S- and M-SWCNTs induced a significant decrease in GSH luminescence activity, with M-SWCNTs B-inducing a small but significant decline compared to S-SWCNTs (figure 4F). We also performed DCF fluorescence assays in THP-1 and BEAS-2B cells, which demonstrated increased ROS generation by M- compared to S-SWCNTs (Figure S4). No differences were observed between M-SWCNTs, P2-SWCNTs, or remixed tubes. All considered, these data demonstrate that in spite of abiotic and cellular differences in the potency of the pro-oxidative SWCNT effects, these dissimilarities do not translate into different levels of IL-1β and TGF-β1 production, suggesting that SWCNT characteristics other than chirality play a dominant role in determining the pro-fibrogenic effects of the tubes. This is in keeping with our previous studies demonstrating that a number of SWCNT properties combine in an integrated fashion to generate biological hazard rather than a single property dominating.[18]

S-SWCNT exert similar pro-fibrogenic effects on the lung as M-SWCNTs

We have previously demonstrated that the aspect ratio, state of aggregation, suspension stability index, hydrophobicity, metal impurities, surface reactivity, surface functionality, and surface coatings contribute in one way or another to the pulmonary hazard potential of SWCNTs.[18] A combination of these properties determine cellular uptake, lysosomal entry, catalytic injury to the lysosome membrane, assembly of the NLRP3 inflammasome and IL-1β production in pulmonary macrophages.[18] Activated macrophages contribute, in turn, to an EMT cascade in which the production of growth factors, like TGF-β1 and PDGF-AA, results in collagen deposition in the lung.[18] To determine to what extent the chirality and electronic properties of SWCNTs play a role in this march of events, oropharyngeal aspiration of S- and M-SWCNTs was used in C57BL/6 mice. The instillation dose was based on the occupational assessment of MWCNT airborne levels in a production facility, where ambient exposure levels as high as 400 $\mu g/m^3$ have been recorded.[32] Using this as the theoretical exposure dose in an adult subject breathing ambient air at 20 L/min and assuming a 30% deposition rate of the tubes during an occupational exposure for 16 weeks (8 h/day, 5 d/week), the total lung burden will be 92.16 mg.[33] Assuming an alveolar surface area of 102 m^2, the equivalent surface area dose can amount to 903.53 $\mu g/m^2$ in the lung of an exposed worker. This equals 1.81 mg/kg in a 25 g mouse with an alveolar epithelial surface area of 0.05 m^2.[34] Accordingly, we decided on a bolus installation dose of 2 mg/kg for each of the

Author Manuscript Author Manuscript Author Manuscript Author Manuscript

materials per animal. The positive control consisted of an oropharyngeal installation of 5 mg/kg Min-U-Sil (α-quartz), a highly inflammogenic material that causes chronic lung inflammation and fibrosis. Animal sacrifice was performed 21 days after exposure. Examination of the bronchoalveolar lavage fluid (BALF) demonstrated non-significant changes in the total and differential counts in animals exposed to the SWCNTs preparations (Figure S5A). Only quartz resulted in a slightly higher neutrophil count after 21 days. Histological examination showed mild pulmonary inflammation in response to quartz and to all of the SWCNT types (Figure S5B). These morphological changes were accompanied by a significant increase in TGF-β1 levels in the BALF for quartz and for all SWCNT types (Figure 5A). However, there were no differences in the extent of pulmonary inflammation or TGF-β1 levels between metallic and semiconducting SWCNTs. Similar observations were made when measuring PDGF-AA: all the SWCNT types induced an indiscriminate increase in PDGF-AA levels in the BALF (Figure 5B). Moreover, while all the tubes and quartz induced increased collagen deposition in the lung as determined by a Sircol assay, we did not observe a significant difference between S- and M-SWCNTs (Figure 5C). This was further confirmed by visualization of the collagen deposition with Masson's trichrome staining, which revealed mild but equivalent amounts of lung fibrosis for S-SWCNTs compared to M-SWCNTs (Figure 5D). Thus, in spite of the differences in the electron transduction capabilities and the pro-oxidative effects of these materials *in vitro*, we did not observe an independent contribution of chirality to the pro-fibrogenic potential of SWCNTs in the lung.

Well-suspended S-SWCNT and M-SWCNT do not induce antibacterial effects in *E. coli*

It was shown previously that aggregated (*i.e.*, bundled) SWCNTs, either in aqueous solution or deposited as thin films, exert anti-bacterial effects in E. *coli* that relates to the electronic properties of the materials.[25]. Not only did metallic tubes show enhanced antibacterial effects compared to semiconducting SWCNTs, but M-SWCNTs also catalyzed increased lipid peroxidation and oxidative stress effects in the bacterial membrane compared to S-SWCNTs. In order to determine if bacteriostatic effects can be demonstrated by our library materials, we performed growth analysis in *E. coli*. Log-phase *E. coli* cultures were inoculated with 12.5–100 μg/mL SWCNTs, and cell densities were monitored for 24 hours. Although a slight but non-significant decline in *E. coli* growth (OD_{600}) was observed for all SWCNT variants (compared to the non-treated controls), there was no significant difference between S- and M-SWCNTs (Figure 6A). In addition to analyzing bacterial growth, we also studied membrane permeability by assaying the culture supernatant for release of β-galactosidase. Triton X-100 was used as a positive control. Interestingly, none of the materials resulted in β-galactosidase release (Figure 6B). In contrast, another carbon allotrope, graphene oxide (GO), was quite effective in permeabilizing the E. *coli* membrane.[35–37] Utilizing propidium iodide (PI) staining and confocal microscopy, we could also demonstrate that increased PI uptake in response to GO was not seen with SWCNTs, irrespective of their electronic properties. GO was also effective in promoting β-galactosidase release (Figure 6C). Additional analysis of E. *coli* morphology using scanning electron microscopy (SEM) confirmed that while GO induced bacterial lysis and membrane damage, none of the SWCNT preparations exerted similar effects (Figure 6D).

Author Manuscript Author Manuscript Author Manuscript Author Manuscript

DISCUSSION

In this study, we performed a comprehensive analysis of the biological impact of highly purified S-SWCNTs and M-SWCNTs on mammalian cells, bacteria, and the rodent lung. We demonstrate that in spite of the lack of cytotoxicity for either SWCNT type, both variants could trigger IL-1β and TGF-β1 production *in vitro* as well as in the mouse lung, in parallel with a mild degree of localized pulmonary fibrosis. However, there was no difference between S- and M-SWCNTs in generating their pro-fibrotic effects in the rodent lung. In contrast to previous accounts of exaggerated antibacterial effects of M- compared to S-SWCNTs, we could not demonstrate any effect on the *E. coli* growth or the membrane integrity, likely as a result of lesser aggregation and a higher level of purity of our sorted SWCNTs. All considered, these data demonstrate that the chirality of SWCNTs and accompanying electronic properties do not make a major independent impact on SWCNT toxicity in the lung, and that the state of dispersal and aggregation of sorted tubes may determine their effects on the bacterial membrane.

We have previously demonstrated that MWCNTs and SWCNTs are capable of exerting hazardous effects in the lung, which can be ascribed to an interdependent set of properties that determine bioavailability, cellular uptake, and subcellular localization in lysosomes, as well as another set of properties that determine catalytic injury to the organellar membrane once taken up by the lysosome.[10,13,15–16,18,38] Thus, while CNT characteristics such as aggregation, hydrophobicity, colloidal stability, charge, aspect ratio, and the protein corona/coating determine sedimentation, bioavailability, and cellular uptake, properties such as length/HAR, charge, surface functionalization, presence of metal impurities, surface reactivity (*e.g.*, based on defects), and ROS generation play a role in damage to the lysosomal membrane. In an attempt to determine to what extent the chirality and electronic properties of SWCNTs contribute to bioavailability and catalytic injury to the lysosomal membrane, it was necessary to refine our purification and suspension methods for high-quality dispersion of metallic and semiconductor tubes in aqueous biological media, where these materials are also free from contaminants that can generate hazardous effects. This necessitated the use of DGU to achieve high purity (>98.5%) populations of metallic and semiconducting SWCNTs. Centrifugation steps during this process remove aggregated SWCNTs, catalysts, and metal contaminants that may have been present in the as-received SWCNT powder. The subsequent flocculation and rinsing of the sorted SWCNT populations also removed detergents and surfactants from the sorted SWCNTs, to the extent that we could not observe membrane lytic effects. The distribution analysis, based on the AFM images, reflects the uniformity of length and diameter of our sorted SWCNTs, in addition to the excellent state of dispersion and colloidal suspension stability in aqueous biological media.

In contrast to the sorted SWCNTs previously prepared to study the electronic properties of SWCNTs in *E. coli*, we did not observe major differences in the pro-fibrogenic effects of M- and S-SWCNTs in the lung.[25] Both SWCNT types, including relevant controls, were taken up in roughly equal amounts in THP-1 cells, with the ability to trigger lysosomal damage and IL-1β production independent of metallic or semiconductor status. While it could clearly be shown that M-SWCNTs are more reactive in abiotic and cellular assays that measure

Author Manuscript Author Manuscript Author Manuscript Author Manuscript

ROS production and GSH depletion, these differential effects did not contribute to significant differences in TGF-β1, PDGF-AA and collagen production *in vivo*. This suggests that while chirality may play a role in the generation of biological responses, electronic properties do not dominate the integrated set of properties that determine outcomes such as bioavailability/cell uptake or catalytic injury to the lysosomal membrane. Moreover, it is important to consider that in addition to the electronic properties of SWCNTs contributing to electron conduction and ROS generation, SWCNTs and MWCNTs are also capable of generating oxygen radicals and oxidative stress as a result of material interactions at the nano/bio interface. These include ROS production as a consequence of NADPH oxidase assembly during phagolysosome uptake, the redox activity of metal impurities, and other less well-defined biological pathways such as triggering of mitochondrial ROS production, *etc*.[38] For the current communication, we can exclude the presence of metal impurities because of the high purity levels and extensive rinsing of our materials. Thus, although chirality and electronic properties contribute to ROS generation, this activity only makes a minor contribution to the integrated set of properties that are ultimately involved in determining oxidative stress and/or triggering of lysosome damage. This does not signify, however, that all semiconductor nanomaterials capable of ROS production, lack the capability of producing biological injury. For instance, we have previously demonstrated that specific transition metal oxide and Pd-doped Co_3O_4 nanoparticles generate acute pro-inflammatory effects in the lung premised on the principles of oxygen radical production as a function of the bandgap energy levels.[31,39] Moreover, the generation of biological injury by engineered nanomaterials is frequently the result of an interrelated set of physicochemical properties that engage adverse outcome pathways (AOP) based on a number of complementary events at the nano/bio interface.[40–47] For SWCNTs and MWCNTs, the reactivity of the carbon surface together with characteristics such as aspect ratio, surface functionality, *etc*., combine in the delivery of injury to the lysosomal membrane, NLRP3 inflammasome assembly, and initiation of an EMT response pathway that leads to lung inflammation and a fibrotic effect. The pro-fibrogenic paradigm allows for a predictive toxicological approach using this AOP.[10,18,38,45–48]

The incongruence of our results with previous studies in *E. coli* using sorted SWCNTs is likely due to differences in approach as well as the purity and dispersion characteristics of the materials being examined. The earlier study demonstrated increased bacterial toxicity, membrane permeability, and oxidative stress in response to sorted SWCNTs that are enriched in the metallic fraction.[25] Moreover, the antibacterial effects involve direct interaction of aggregated M-SWCNTs with the bacterial membrane, either under the form or aqueous suspension conditions.[25] Not only did we use materials with a higher degree of purity, but also prepared tubes that were better dispersed and exhibiting a high colloidal stability in aqueous suspension. While our purified materials were taken up by mammalian cells, with the ability to induce adverse biological responses, we did not observe an effect on *E. coli* as determined by bacterial growth, membrane permeability, and morphological analysis. While we lack a direct explanation for the lack of a response outcome in bacteria with our materials, it is possible that the state of aggregation and attachment efficiency of less dispersed tubes could be more prone to damage the bacterial membrane. It is also

Author Manuscript Author Manuscript Author Manuscript Author Manuscript

possible that presence of impurities, such as detergents that were not thoroughly cleaned away, could have had an impact on the bacterial membrane in previous studies.

Our study is of considerable importance from a regulatory perspective, because highly purified SWCNT preparations are increasingly being used for electronic applications. This could translate into the increased likelihood of exposure in workers and consumers. Moreover, the regulatory agencies may have to consider whether it is necessary to require independent safety assessment of SWCNT electronic properties, particularly if it is a high metallic or semiconductor purity level is considered as introducing a new chemical composition. It may be necessary, therefore, to consider metallic and semiconducting properties independent of tube categories, such as single walled *vs.* multi walled, purified *vs.* crude, functionalized *vs.* non-functionalized tubes, *etc.* Our study of electronic sorted SWCNTs suggest that metallic and semiconducting tubes do not generate disparate effects in the lung compared to unsorted SWCNTs. Thus, there may be no immediate requirement to include chirality as an independent SWCNT category. However, this position may change if exposure monitoring should reveal differences in the aerosolized behavior of the sorted tubes or when production volumes increase above a certain threshold. Under those circumstances, it may be deemed necessary to require additional information about the contribution of chirality to the traditional set of physicochemical properties that are being assessed. In the interim, however, it is important to continue all engineering and personal protective measures to protect people working with SWCNTs. If further studies determine that metallic SWCNTs do pose increased hazard on environmental organisms such as bacteria, it may also be necessary to conduct more elaborate studies on the environmental behavior of sorted SWCNTs.

CONCLUSION

In summary, we demonstrate that in spite of increased pro-oxidative effects of metallic *versus* semiconducting SWCNTs under abiotic and cellular conditions, there are no differences in the hazard potential of these materials when assessed for their pro-fibrogenic effects in the lung. Moreover, in spite of previous studies showing that metallic are more toxic than semiconducting SWCNTs in *E. coli*, our study did not demonstrate an effect on bacterial viability or membrane permeability under aqueous suspension conditions. Our data indicate that highly purified, electronic-sorted SWCNTs do not show significant differences in their hazard potential in the lung. Currently, there appears to be no necessity to use chirality as an independent category for regulatory purposes. These results will also be of significant interest to those interested in using sorted SWCNTs for commercial purposes.

METHODS/EXPERIMENTAL

Source and Preparation of Sorted SWCNTs

The methodology for detailed characterization of electronic sorted SWCNTs is described in the Supporting Information *via* the Internet at http://pubs.acs.org. Briefly, P2 SWCNTs (Carbon Solutions, Inc.) were sorted into metallic and semiconducting species using density gradient ultracentrifugation, using a modification of the previously described method. [2,14]

Author Manuscript Author Manuscript Author Manuscript Author Manuscript

Preparation of Nanomaterial Suspensions and Cell Culture with Semiconducting and Metallic SWCNTs

Semiconducting and metallic SWCNT stock solutions were first prepared in DI H_2O at 1 mg/mL. BEAS-2B and THP-1 cells were obtained from ATCC (Manassas, VA). 1×10^4 BEAS-2B cells were cultured in 0.1 mL BEGM in 96-well plates at 37 °C. THP-1 cells were pretreated with 1 μg/mL phorbol 12-myristate acetate (PMA) overnight and primed with 10 ng/mL lipopolysaccharide (LPS). Aliquots of 3×10^4 primed cells were cultured in 0.1 mL medium with carbon nanotubes in 96-well plates (Costar, Corning, NY, USA) at 37 °C for 24 h. In order to provide less aggregated tubes that can be suspended in biological aqueous media, all the SWCNT suspensions were freshly prepared by adding the stock solutions to BEGM or RPMI 1640 media at 12.5–100 μg/mL in the presence of BSA (0.6 mg/mL) and DPPC (0.01 mg/mL). After 24 h of culture, the supernatants were collected for the measurement of IL-1β (BD Biosciences, San Diego, CA) and TGF-β1 (Promega, Madison, WI) using ELISA kits according to manufacturer's instructions. Concentrations are expressed as pg/mL.

Cytotoxicity Assessment

Cytotoxicity was determined by a MTS assay, which was carried out with CellTiter 96 Aqueous (Promega Corp.) kit. 1×10^4 BEAS-2B or 3×10^4 THP-1 cells in 100 μL of culture medium were plated in each well of 96 multiwell plates (Costar, Corning, NY) for overnight growth. The medium was removed, and cells were treated for 24 h with 100 μL of 12.5–100 μg/mL SWCNT suspensions. After the treatment, the cell culture medium was removed and followed by washing three times with PBS. Each well received 120 μL of culture medium containing 16.7 % of MTS stock solution for 1 h at 37 °C in a humidified 5 % CO_2 incubator. The plate was centrifuged at 2000 g for 10 min in NI Eppendorf 5430 with a microplate rotor to spin down the cell debris. An 85 μL aliquot of the supernatant was removed from each well and transferred into a new 96 multiwell plate. The absorbance of formazan was read at 490 nm on a SpectraMax M5 microplate reader (Molecular Devices Corp., Sunnyvale, CA, USA).

Mouse Exposures and Outcome Assessment

Eight-week-old male C57Bl/6 mice were purchased from Charles River Laboratories (Hollister, CA). All animals were housed under standard laboratory conditions according to UCLA guidelines for care and treatment as well as the NIH Guide for the Care and Use of Laboratory Animals in Research (DHEW78–23). The animal experiments were approved by the Chancellor's Animal Research Committee at UCLA and include standard operating procedures for animal housing (filter-topped cages; room temperature at 23 ± 2 °C; 60 % relative humidity; 12 h light, 12 h dark cycle) and hygiene status (autoclaved food and acidified water). Animal exposures to nanomaterials were carried out by an oropharyngeal aspiration method developed at NIOSH. The animals received oropharyngeal aspiration of semiconducting-, metallic-, semiconducting + metallic and P2-SWCNTs nanomaterial suspensions at 2 mg/Kg at the back of the tongue. The mice were sacrificed after 21 days to assess sub-chronic effects. The bronchoalveolar lavage fluid (BALF) and lung tissue were collected for measurement of TGF-β1 and PDGF-AA levels and performance of

Author Manuscript Author Manuscript Author Manuscript Author Manuscript

Hematoxylin and Eosin (H&E) or Masson's trichrome staining. The detailed protocol is described in the Supporting Information.

Determination of Bacteria Viability and β-Galactosidase Release in Response to SWCNT Exposure

The *E. coli* strain, ATCC 25922, was used for these studies. A growth inhibition curve was established to assess the possible bacteriostatic effect of SWCNTs. Bacterial membrane permeability was evaluated by measuring β-galactosidase release with a Beta-Glo® Assay System (Promega). The detailed protocol is described in the Supporting Information.

Statistical Analysis

Mean and standard deviation (SD) were calculated for each parameter. Results were expressed as mean ± SD of multiple determinations. Comparisons within each group were conducted by a two-sided Student's t test. A statistically significant difference was assumed with $p < 0.05$.

Supplementary Material

Refer to Web version on PubMed Central for supplementary material.

Acknowledgments

Research reported in this publication was supported by the National Institute of Environmental Health Sciences of the National Institutes of Health under Award Number RO1ES022698. The content is solely the responsibility of the authors and does not necessarily represent the official views of the National Institutes of Health. This study is also based upon work supported by the National Science Foundation and the Environmental Protection Agency under Award No. DBI-1266377. Fluorescent microscopy was performed at the CNSI Advanced Light Microscopy/ Spectroscopy Shared Facility at UCLA.

References

1. Geier ML, McMorrow JJ, Xu WC, Zhu J, Kim CH, Marks TJ, Hersam MC. Solution-Processed Carbon Nanotube Thin-Film Complementary Static Random Access Memory. Nat Nanotechnol. 2015; 10:944–948. [PubMed: 26344184]
2. Arnold MS, Green AA, Hulvat JF, Stupp SI, Hersam MC. Sorting Carbon Nanotubes by Electronic Structure Using Density Differentiation. Nat Nanotechnol. 2006; 1:60–65. [PubMed: 18654143]
3. Charlier JC, Blase X, Roche S. Electronic and Transport Properties of Nanotubes. Rev Mod Phys. 2007; 79:677–732.
4. Hong S, Myung S. Nanotube electronics - A Flexible Approach to Mobility. Nat Nanotechnol. 2007; 2:207–208. [PubMed: 18654263]
5. Hersam MC. Progress Towards Monodisperse Single-Walled Carbon Nanotubes. Nat Nanotechnol. 2008; 3:387–394. [PubMed: 18654561]
6. Shvedova AA, Kisin E, Murray AR, Johnson VJ, Gorelik O, Arepalli S, Hubbs AF, Mercer RR, Keohavong P, Sussman N, et al. Inhalation *vs.* Aspiration Of Single-Walled Carbon Nanotubes in C57BL/6 Mice: Inflammation, Fibrosis, Oxidative Stress, And Mutagenesis. Am J Physiol-Lung C. 2008; 295:L552–L565.
7. Warheit DB, Laurence BR, Reed KL, Roach DH, Reynolds GAM, Webb TR. Comparative Pulmonary Toxicity Assessment of Single-Wall Carbon Nanotubes in Rats. Toxicol Sci. 2004; 77:117–125. [PubMed: 14514968]

Author Manuscript Author Manuscript Author Manuscript Author Manuscript

8. Jia G, Wang HF, Yan L, Wang X, Pei RJ, Yan T, Zhao YL, Guo XB. Cytotoxicity of Carbon Nanomaterials: Single-Wall Nanotube, Multi-Wall Nanotube, and Fullerene. Environ Sci Technol. 2005; 39:1378–1383. [PubMed: 15787380]
9. Kayat J, Gajbhiye V, Tekade RK, Jain NK. Pulmonary Toxicity of Carbon Nanotubes: A Systematic Report. Nanomed-Nanotechnol. 2011; 7:40–49.
10. Li RB, Wang X, Ji ZX, Sun BB, Zhang HY, Chang CH, Lin SJ, Meng H, Liao YP, Wang MY, et al. Surface Charge and Cellular Processing of Covalently Functionalized Multiwall Carbon Nanotubes Determine Pulmonary Toxicity. ACS nano. 2013; 7:2352–2368. [PubMed: 23414138]
11. Shvedova AA, Kisin ER, Mercer R, Murray AR, Johnson VJ, Potapovich AI, Tyurina YY, Gorelik O, Arepalli S, Schwegler-Berry D, et al. Unusual Inflammatory and Fibrogenic Pulmonary Responses to Single-Walled Carbon Nanotubes in Mice. Am J Physiol-Lung C. 2005; 289:L698–L708.
12. Wang X, Jia G, Wang H, Nie H, Yan L, Deng XY, Wang S. Diameter Effects on Cytotoxicity of Multi-Walled Carbon Nanotubes. J Nanosci Nanotechno. 2009; 9:3025–3033.
13. Mutlu GM, Budinger GRS, Green AA, Urich D, Soberanes S, Chiarella SE, Alheid GF, McCrimmon DR, Szleifer I, Hersam MC. Biocompatible Nanoscale Dispersion of Single-Walled Carbon Nanotubes Minimizes *in vivo* Pulmonary Toxicity. Nano Lett. 2010; 10:1664–1670. [PubMed: 20377197]
14. Nagai H, Okazaki Y, Chew SH, Misawa N, Yamashita Y, Akatsuka S, Ishihara T, Yamashita K, Yoshikawa Y, Yasui H, et al. Diameter and Rigidity of Multiwalled Carbon Nanotubes Are Critical Factors in Mesothelial Injury and Carcinogenesis. P Natl Acad Sci USA. 2011; 108:E1330–E1338.
15. Wang X, Xia T, Duch MC, Ji ZX, Zhang HY, Li RB, Sun BB, Lin SJ, Meng H, Liao YP, et al. Pluronic F108 Coating Decreases the Lung Fibrosis Potential of Multiwall Carbon Nanotubes by Reducing Lysosomal Injury. Nano Lett. 2012; 12:3050–3061. [PubMed: 22546002]
16. Wang X, Xia T, Ntim SA, Ji Z, Lin S, Meng H, Chung C, George S, Zhang H, Wang M, et al. Dispersal State of Multi-walled Carbon Nanotubes Elicits Pro-Fibrogenic Cellular Responses that Correlate with Fibrogenesis Biomarkers and Fibrosis in the Murine Lung. ACS nano. 2011; 5:9772–9787. [PubMed: 22047207]
17. Wang X, Xia T, Ntim SA, Ji ZX, George S, Meng H, Zhang H, Castranova V, Mitra S, Nel AE. Quantitative Techniques for Assessing and Controlling the Dispersion and Biological Effects of Multiwalled Carbon Nanotubes in Mammalian Tissue Culture Cells. ACS nano. 2010; 4:7241–7252. [PubMed: 21067152]
18. Wang X, Duch MC, Mansukhani N, Ji ZX, Liao YP, Wang MY, Zhang HY, Sun BB, Chang CH, Li RB, et al. Use of a Pro-Fibrogenic Mechanism-Based Predictive Toxicological Approach for Tiered Testing and Decision Analysis of Carbonaceous Nanomaterials. ACS nano. 2015; 9:3032–3043. [PubMed: 25646681]
19. Sun BB, Wang X, Ji ZX, Li RB, Xia T. NLRP3 Inflammasome Activation Induced by Engineered Nanomaterials. Small. 2013; 9:1595–1607. [PubMed: 23180683]
20. Fubini B, Ghiazza M, Fenoglio I. Physico-chemical Features of Engineered Nanoparticles Relevant to Their Toxicity. Nanotoxicology. 2010; 4:347–363. [PubMed: 20858045]
21. Ge CC, Meng L, Xu LG, Bai R, Du JF, Zhang LL, Li Y, Chang YZ, Zhao YL, Chen CY. Acute Pulmonary and Moderate Cardiovascular Responses of Spontaneously Hypertensive Rats After Exposure to Single-Wall Carbon Nanotubes. Nanotoxicology. 2012; 6:526–542. [PubMed: 21657814]
22. Liu Y, Zhao YL, Sun BY, Chen CY. Understanding the Toxicity of Carbon Nanotubes. Accounts Chem Res. 2013; 46:702–713.
23. Kagan V, Potapovich A, Osipov A, Schwegler-Berry D, Kisin E, Mercer R, Castranova V, Shvedova A. Iron-Rich Single Walled Carbon Nanotubes Are Effective Catalysts of Oxidative Stress in Raw 264.7 Macrophage Cell Culture Model: Interactions With Inflammatory Response and *In Vivo* Implications. Free Radical Bio Med. 2004; 37:S51–S52.
24. Wang X, Guo J, Chen T, Nie HY, Wang HF, Zang JJ, Cui XX, Jia G. Multi-walled Carbon Nanotubes Induce Apoptosis *via* Mitochondrial Pathway and Scavenger Receptor. Toxicology in Vitro. 2012; 26:799–806. [PubMed: 22664788]

Author Manuscript Author Manuscript Author Manuscript Author Manuscript

25. Vecitis CD, Zodrow KR, Kang S, Elimelech M. Electronic-Structure-Dependent Bacterial Cytotoxicity of Single-Walled Carbon Nanotubes. ACS nano. 2010; 4:5471–5479. [PubMed: 20812689]
26. Antaris AL, Seo JWT, Green AA, Hersam MC. Sorting Single-Walled Carbon Nanotubes by Electronic Type Using Nonionic, Biocompatible Block Copolymers. ACS nano. 2010; 4:4725–4732. [PubMed: 20669897]
27. Yazdi AS, Guarda G, Riteau N, Drexler SK, Tardivel A, Couillin I, Tschopp J. Nanoparticles Activate the NLR Pyrin Domain Containing 3 (NLRP3) Inflammasome and Cause Pulmonary Inflammation Through Release of IL-1 Alpha and IL-1 Beta. P Natl Acad Sci USA. 2010; 107:19449–19454.
28. Ji Z, Wang X, Zhang H, Lin S, Meng H, Sun B, George S, Xia T, Nel AE, Zink JI. Designed Synthesis of CeO_2 Nanorods and Nanowires for Studying Toxicological Effects of High Aspect Ratio Nanomaterials. ACS nano. 2012; 6:5366–5380. [PubMed: 22564147]
29. Lin SJ, Wang X, Ji ZX, Chang CH, Dong Y, Meng H, Liao YP, Wang MY, Song TB, Kohan S, et al. Aspect Ratio Plays a Role in the Hazard Potential of CeO_2 Nanoparticles in Mouse Lung and Zebrafish Gastrointestinal Tract. ACS nano. 2014; 8:4450–4464. [PubMed: 24720650]
30. Mercer RR, Scabilloni J, Wang L, Kisin E, Murray AR, Schwegler-Berry D, Shvedova AA, Castranova V. Alteration of Deposition Pattern and Pulmonary Response As A Result of Improved Dispersion of Aspirated Single-Walled Carbon Nanotubes in A Mouse Model. Am J Physiol-Lung C. 2008; 294:L87–L97.
31. Zhang HY, Pokhrel S, Ji ZX, Meng H, Wang X, Lin SJ, Chang CH, Li LJ, Li RB, Sun BBW, et al. PdO Doping Tunes Band-Gap Energy Levels as Well as Oxidative Stress Responses to a Co_3O_4 p-Type Semiconductor in Cells and the Lung. J Am Chem Soc. 2014; 136:6406–6420. [PubMed: 24673286]
32. Han JH, Lee EJ, Lee JH, So KP, Lee YH, Bae GN, Lee SB, Ji JH, Cho MH, Yu IJ. Monitoring Multiwalled Carbon Nanotube Exposure in Carbon Nanotube Research Facility. Inhal Toxicol. 2008; 20:741–749. [PubMed: 18569096]
33. Galer DM, Leung HW, Sussman RG, Trzos RJ. Scientific and Practical Considerations for the Development of Occupational Exposure Limits (OELs) for Chemical-Substances. Regul Toxicol Pharm. 1992; 15:291–306.
34. Stone KC, Mercer RR, Gehr P, Stockstill B, Crapo JD. Allometric Relationships of Cell Numbers and Size in the Mammalian Lung. Am J Resp Cell Mol. 1992; 6:235–243.
35. Akhavan O, Ghaderi E. Toxicity of Graphene and Graphene Oxide Nanowalls Against Bacteria. ACS nano. 2010; 4:5731–5736. [PubMed: 20925398]
36. Liu SB, Hu M, Zeng TH, Wu R, Jiang RR, Wei J, Wang L, Kong J, Chen Y. Lateral Dimension-Dependent Antibacterial Activity of Graphene Oxide Sheets. Langmuir. 2012; 28:12364–12372. [PubMed: 22827339]
37. Perreault F, de Faria AF, Nejati S, Elimelech M. Antimicrobial Properties of Graphene Oxide Nanosheets: Why Size Matters. ACS nano. 2015; 9:7226–7236. [PubMed: 26091689]
38. Sun BB, Wang X, Ji ZX, Wang MY, Liao YP, Chang CH, Li RB, Zhang HY, Nel AE, Xia T. NADPH Oxidase-Dependent NLRP3 Inflammasome Activation and Its Important Role in Lung Fibrosis by Multiwalled Carbon Nanotubes. Small. 2015; 11:2087–2097. [PubMed: 25581126]
39. Zhang HY, Ji ZX, Xia T, Meng H, Low-Kam C, Liu R, Pokhrel S, Lin SJ, Wang X, Liao YP, et al. Use of Metal Oxide Nanoparticle Band Gap To Develop a Predictive Paradigm for Oxidative Stress and Acute Pulmonary Inflammation. ACS nano. 2012; 6:4349–4368. [PubMed: 22502734]
40. Silva RM, Doudrick K, Franzi LM, Teesy C, Anderson DS, Wu ZQ, Mitra S, Vu V, Dutrow G, Evans JE, et al. Instillation *versus* Inhalation of Multiwalled Carbon Nanotubes: Exposure-Related Health Effects, Clearance, and the Role of Particle Characteristics. ACS nano. 2014; 8:8911–8931. [PubMed: 25144856]
41. Ge CC, Tian J, Zhao YL, Chen CY, Zhou RH, Chai ZF. Towards Understanding of Nanoparticle-Protein Corona. Arch Toxicol. 2015; 89:519–539. [PubMed: 25637415]
42. Gagner JE, Shrivastava S, Qian X, Dordick JS, Siegel RW. Engineering Nanomaterials for Biomedical Applications Requires Understanding the Nano-Bio Interface: A Perspective. J Phys Chem Lett. 2012; 3:3149–3158. [PubMed: 26296021]

Author Manuscript Author Manuscript Author Manuscript Author Manuscript

43. Nel AE, Madler L, Velegol D, Xia T, Hoek EMV, Somasundaran P, Klaessig F, Castranova V, Thompson M. Understanding Biophysicochemical Interactions at the Nano-Bio Interface. Nat Mater. 2009; 8:543–557. [PubMed: 19525947]

44. Zhu MT, Nie GJ, Meng H, Xia T, Nel A, Zhao YL. Physicochemical Properties Determine Nanomaterial Cellular Uptake, Transport, and Fate. Accounts Chem Res. 2013; 46:622–631.

45. Labib S, Williams A, Yauk CL, Nikota JK, Wallin H, Vogel U, Halappanavar S. Nano-Risk Science: Application of Toxicogenomics in An Adverse Outcome Pathway Framework for Risk Assessment of Multi-Walled Carbon Nanotubes. Part Fibre Toxicol. 2016:13. [PubMed: 26956024]

46. Vietti G, Ibouraadaten S, Palmai-Pallag M, Yakoub Y, Piret JP, Marbaix E, Lison D, van den Brule S. Towards Predicting the Lung Fibrogenic Activity of MWCNT: Key Role of Endocytosis, Kinase Receptors and ERK 1/2 Signaling. Nanotoxicology. 2016; 10:488–500. [PubMed: 26444902]

47. Vietti G, Lison D, van den Brule S. Mechanisms of Lung Fibrosis Induced By Carbon Nanotubes: Towards an Adverse Outcome Pathway (AOP). Part Fibre Toxicol. 2016; 13:11. [PubMed: 26926090]

48. Hussain S, Sangtian S, Anderson SM, Snyder RJ, Marshburn JD, Rice AB, Bonner JC, Garantziotis S. Inflammasome Activation in Airway Epithelial Cells After Multi-Walled Carbon Nanotube Exposure Mediates A Profibrotic Response in Lung Fibroblasts. Part Fibre Toxicol. 2014:11. [PubMed: 24529161]

Author Manuscript Author Manuscript Author Manuscript Author Manuscript

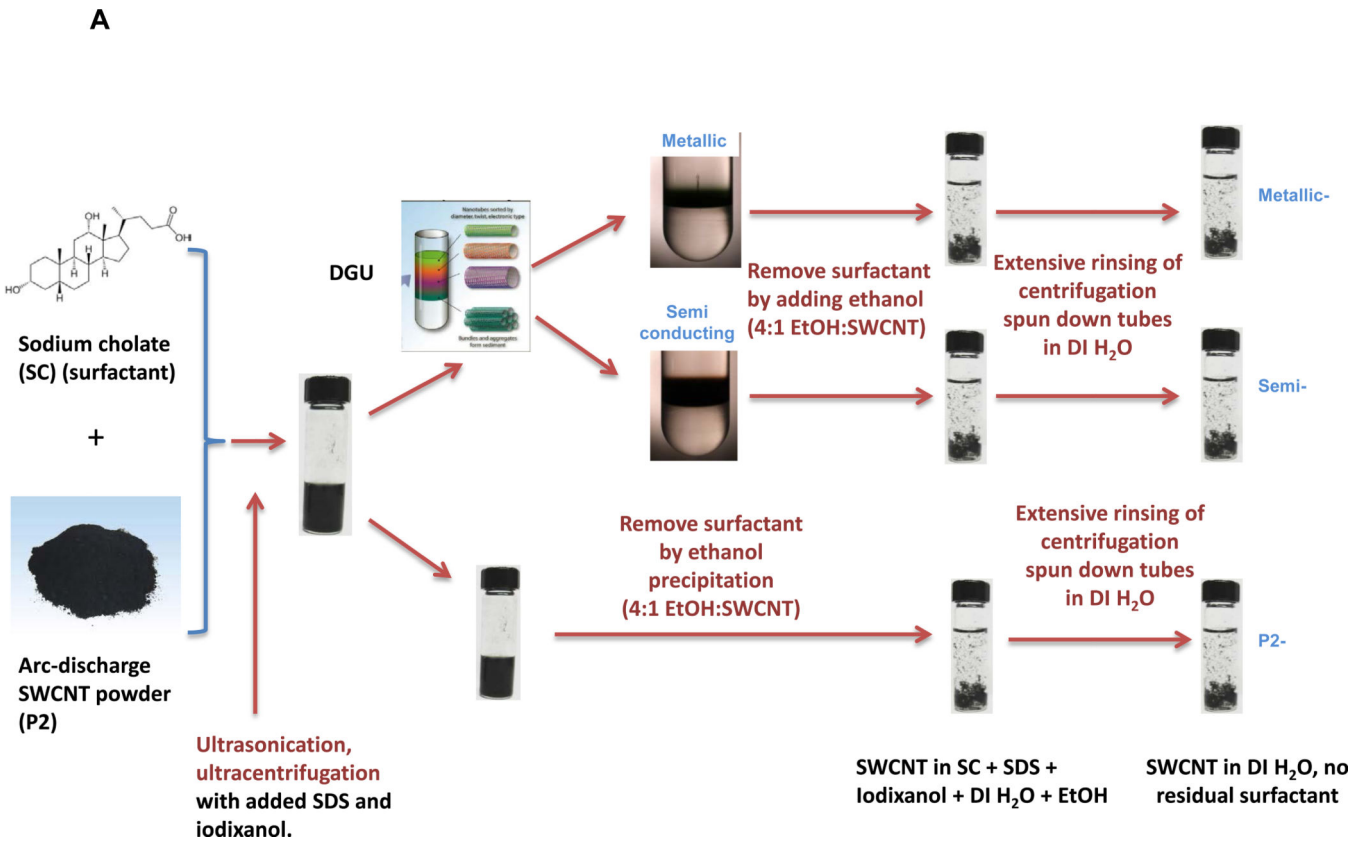

Author Manuscript Author Manuscript Author Manuscript Author Manuscript

B

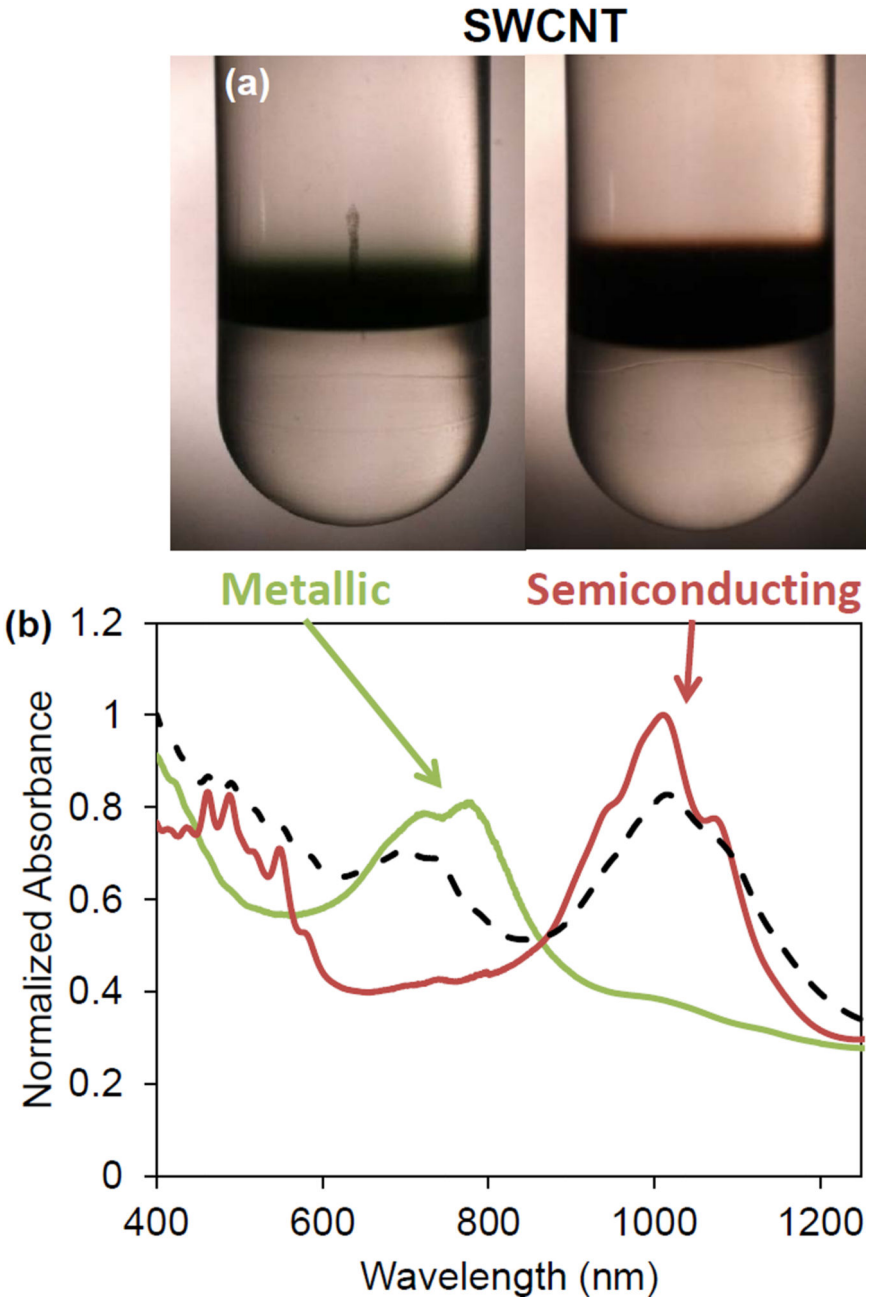

Author Manuscript Author Manuscript Author Manuscript Author Manuscript

C

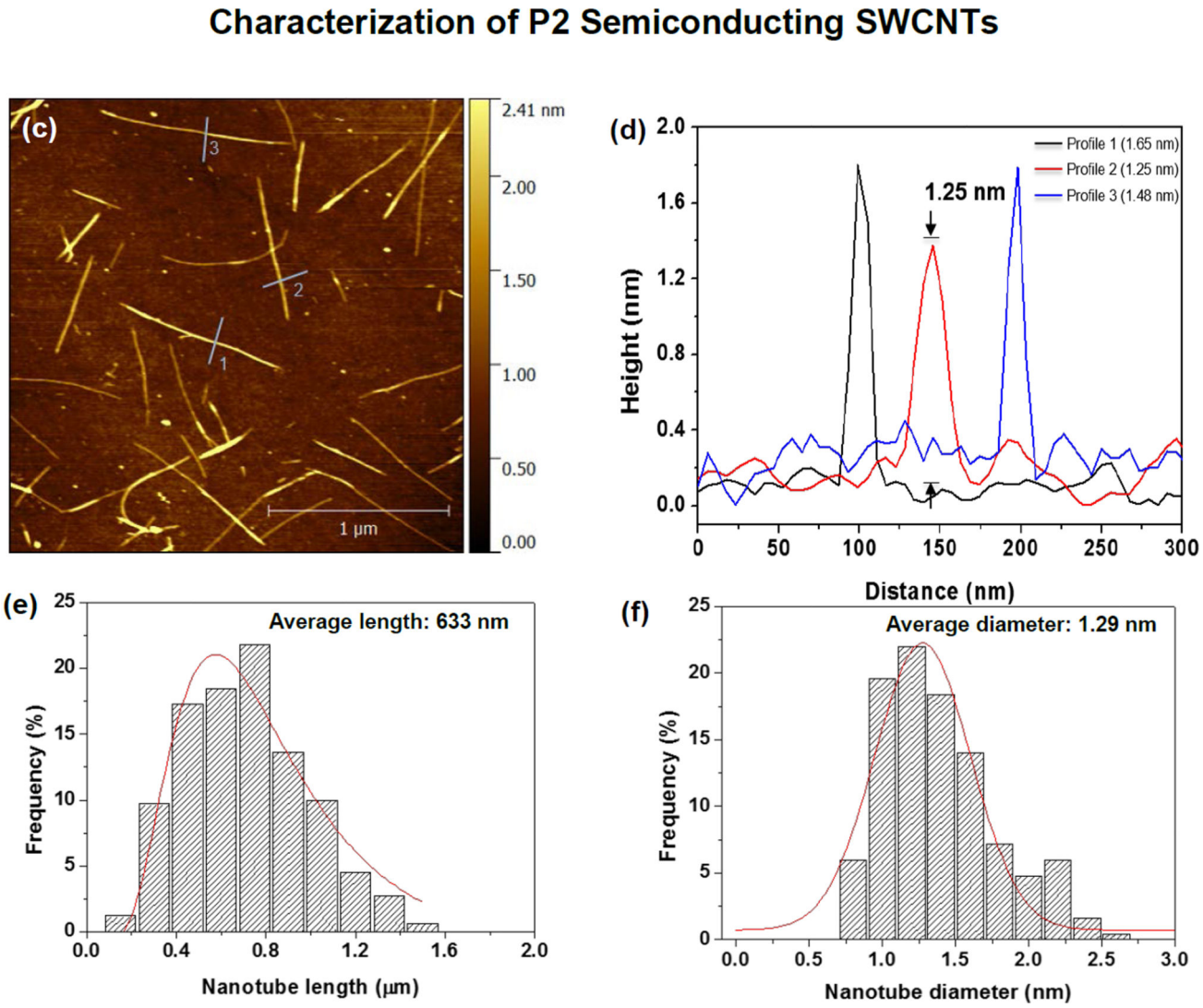

Author Manuscript Author Manuscript Author Manuscript Author Manuscript

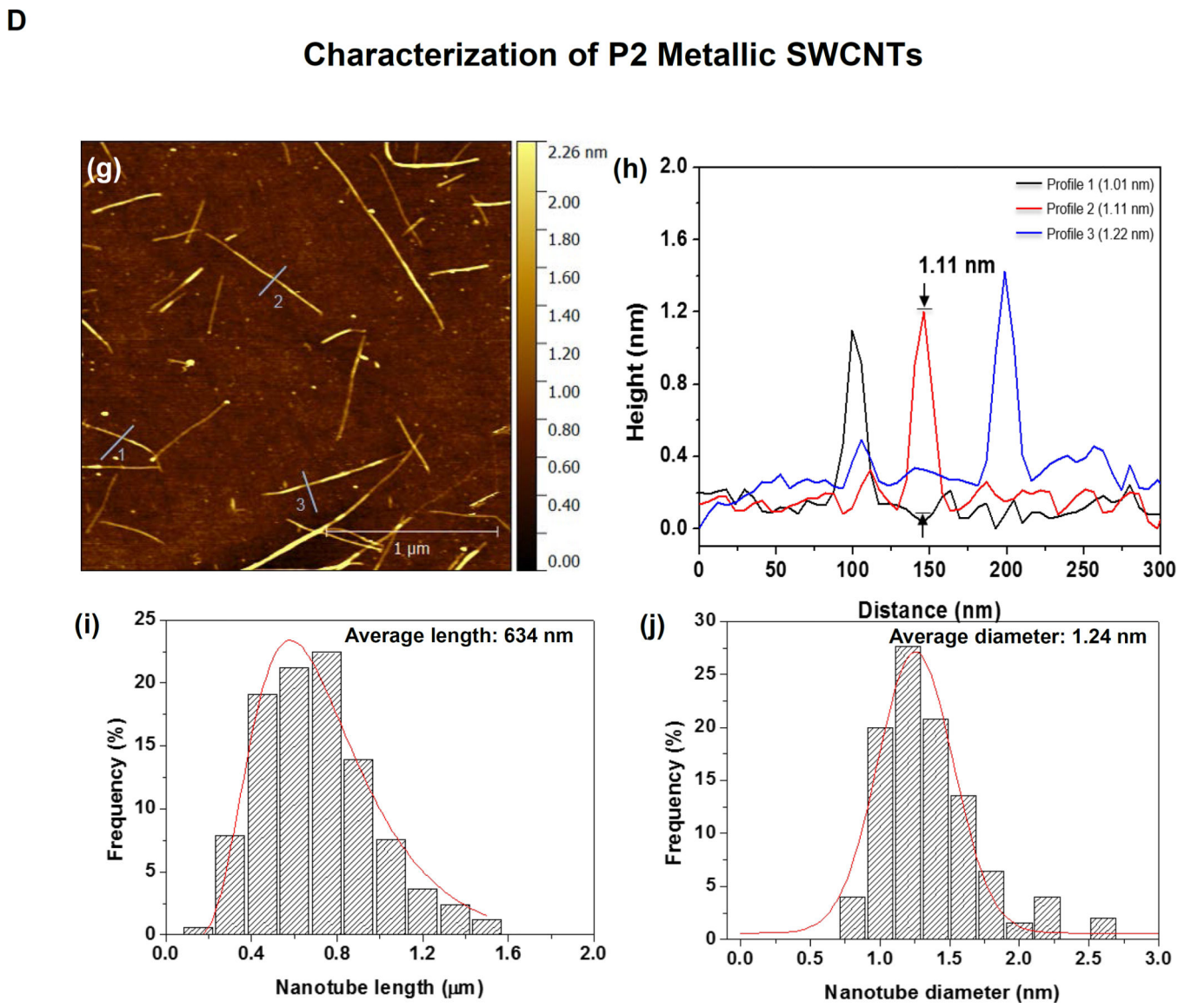

Figure 1. Scheme and characterization of the electronic sorted SWCNTs

(A) Scheme for the preparation of electronic sorted SWCNTs. P2 SWCNTs were sorted into metallic and semiconducting species using density gradient ultracentrifugation (DGU) methods. Briefly, a P2 SWCNTs stock solution was prepared by dispersing the tubes in an aqueous solution containing 1% w/v sodium cholate (SC) followed by 1 h ultrasonication. The stock suspension was then centrifuged at 7500 rpm for 10 min in the presence of sodium dodecyl sulfate (SDS) and SC (SDS:SC ratios of 3:2 *vs.* 1:4 were used for metallic and semiconducting sorting, respectively) to remove large aggregates. The remaining supernatant was for DGU sorting, using iodixanol to make the gradients. After the dispersion was centrifuged at 32,000 rpm for 18 h, 0.25 mm fractions of the supernatant was collected as either metallic or semiconducting tubes. The detailed methodology appear in the Supporting Information. (B) Characterization of the sorted SWCNTs. Photograph of the DGU separation tube (a) and corresponding optical absorption spectra (b). The purity of the final dispersions were >98.8% for M-SWCNT and >98.5% for S-SWCNT as determined by

optical absorbance spectroscopy. (C and D) Characterization of semiconducting (C) and metallic (D) SWCNTs by AFM and optical absorption spectroscopy. Panels (c) and (g) show the AFM images, panels (d) and (h) show the optical absorption spectra, panels (e) and (i) show length distributions, while panels (f) and (j) show the diameter distributions.

Author Manuscript Author Manuscript Author Manuscript Author Manuscript

Author Manuscript Author Manuscript Author Manuscript Author Manuscript

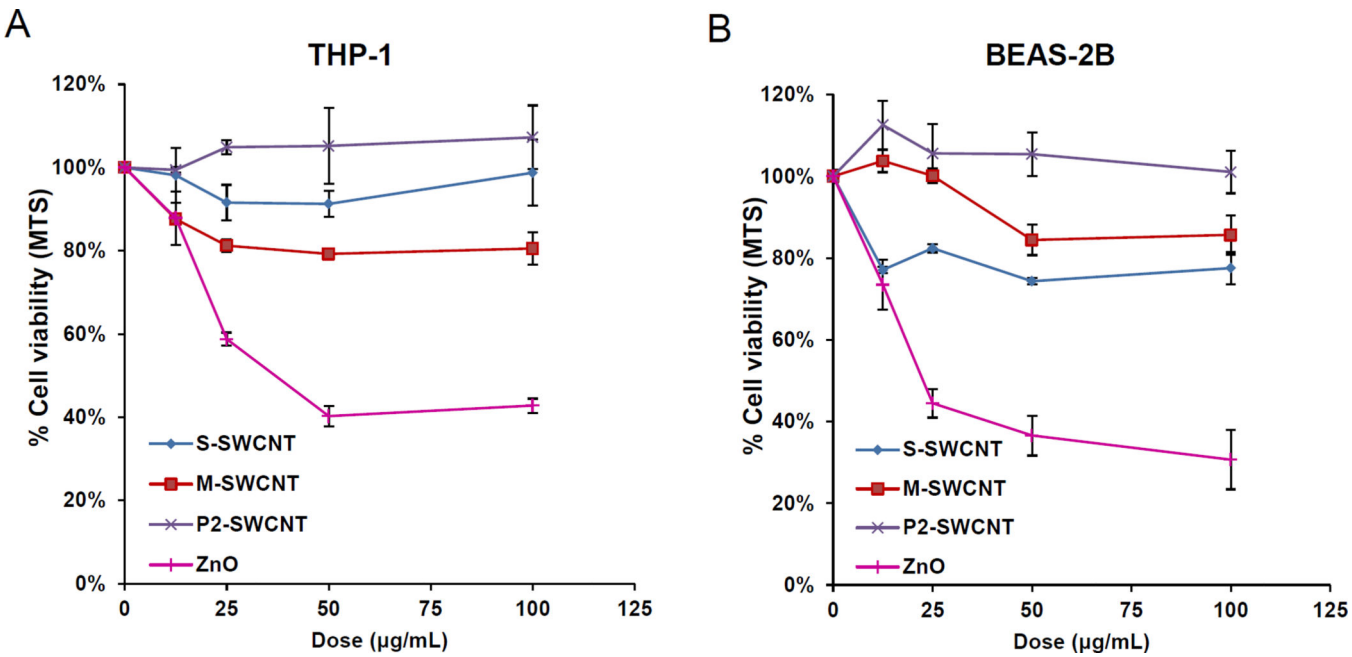

Figure 2. Cytotoxicity in THP-1 and BEAS-2B cells exposed to electronic-sorted SWNCTs

Assessment of cytotoxicity of SWNCTs in (A) THP-1 and (B) BEAS-2B cells. Both cell types were grown in 96-well plates, followed by exposure to 12.5, 25, 50 and 100 μg/mL of each of the SWNCTs suspensions for 24 h. The media were subsequently washed with PBS and replaced with 120 μL aliquots of the MTS working solution. After incubation for 1 hour, the plates were centrifuged to collect the supernatants, and their absorbance read at 490 nm in a microplate reader (SpectroMax M5e, Molecular Devices, Sunnyvale, CA). All the MTS values were normalized according to the nontreated control, which was regarded as representing 100% cell viability. *$p < 0.05$ compared to control.

Author Manuscript Author Manuscript Author Manuscript Author Manuscript

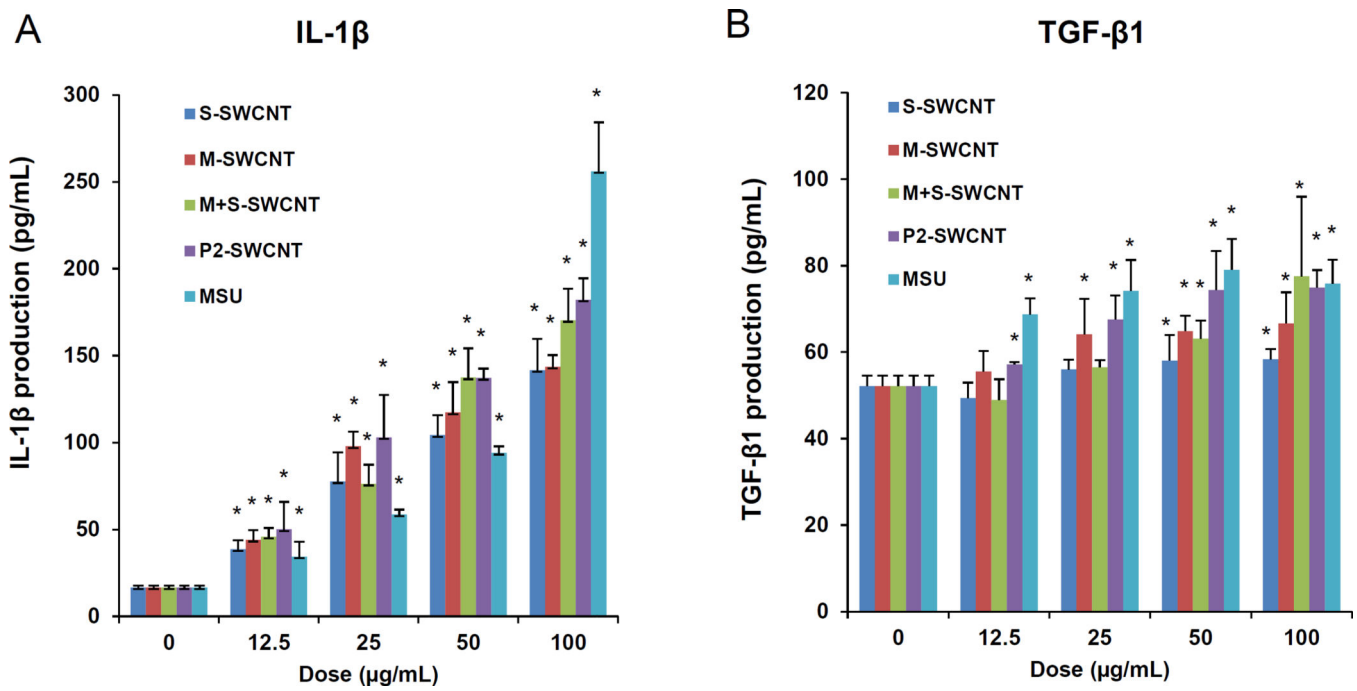

Figure 3. Comparative pro-fibrogenic effects, as reflected by IL-1β and TGF-β1 production in THP-1 and BEAS-2B cells

Cells were exposed to the indicated concentrations of the sorted SWCNTs for 24 h. IL-1β (A) and TGF-β1 (B) levels were determined on the culture supernatants by ELISA. *p< 0.05 compared to control.

Author Manuscript Author Manuscript Author Manuscript Author Manuscript

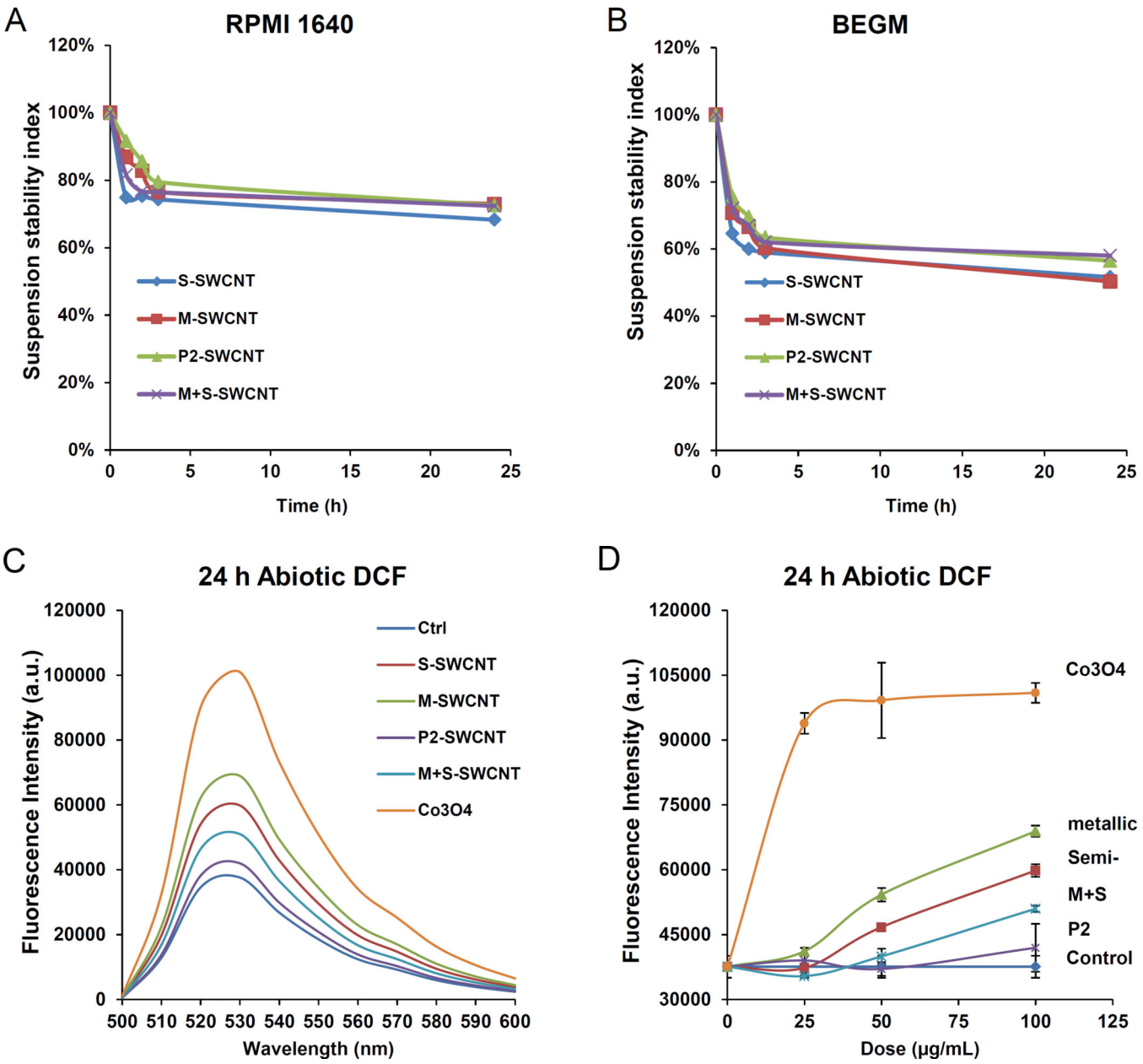

Author Manuscript Author Manuscript Author Manuscript Author Manuscript

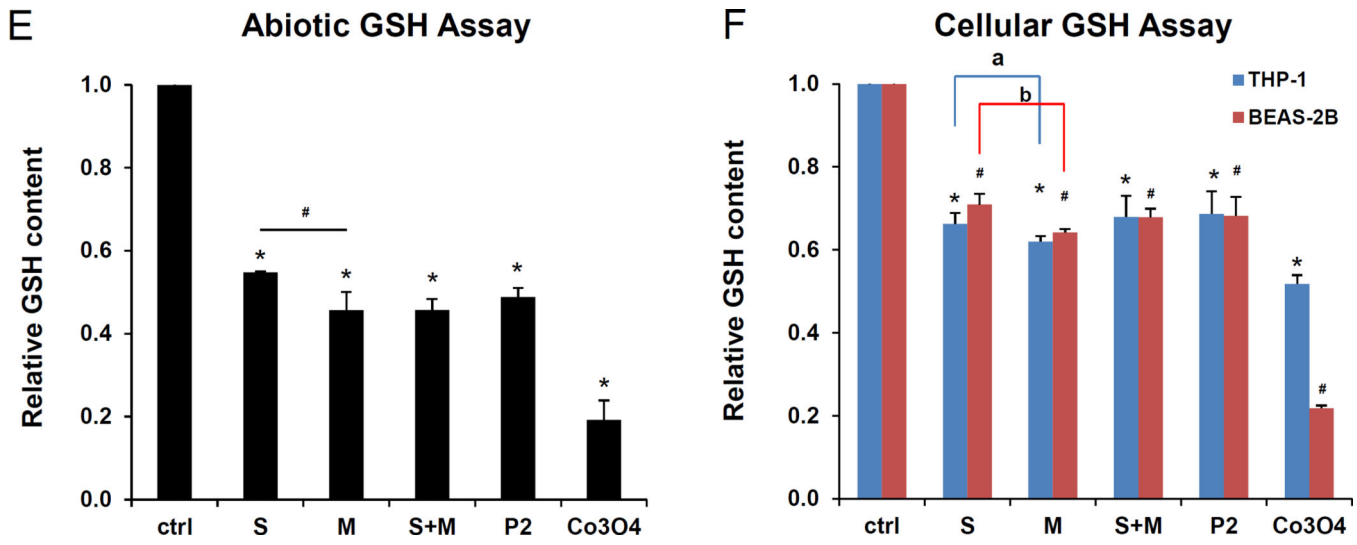

Figure 4. SWCNT suspension stability indices in cell culture media as well as assessment of the material pro-oxidant potential

(A) The SWCNTs were added to RPMI 1640 at 50 μg/mL. The suspension stability index was determined by comparing the initial absorbance (t = 0) to the absorbance at 1, 2, 3, or 24 h. The absorbance measurements were carried out at λ = 550 nm in a SpectroMax M5e (Molecular Devices Corp., Sunnyvale, CA). (B) Similar assessment in BEGM. (C) DCF fluorescence spectroscopy: 29 μmol/L DCF was added to tube suspensions at 12.5–100 μg/mL for 24h, and emission spectra collected at 500−600 nm, with excitation at 490 nm. Both S- and M-SWCNTs showed significant enhancement of DCF fluorescence compared to the non-treated control. ROS production by Co_3O_4 NPs at 100 μg/mL was used as positive control. (D) Comparative expression of the fluorescence intensity at 528 nm demonstrated a proportionally bigger dose-dependent increase in fluorescence activity with metallic compared to semiconducting SWCNTs. (E) Abiotic GSH depletion: 62.5 μmol/L GSH was incubated with 100 μg/mL SWCNTs for 24 h, and the GSH level was determined by the luminescence-based GSH-Glo kit. * $p < 0.05$, compared to control; # $p < 0.05$ compared between S- and M-SWCNTs. (F) Cellular GSH depletion in THP-1 and BEAS-2B cells was determined by the same assay. Both cell types were exposed to SWCNTs at 100 μg/mL for 24 h. GSH abundance was calculated as the fractional luminescence intensity of treated vs. non-treated cells (in which the abundance was regarded as 1.0). * # $p < 0.05$, compared to control (* is for THP-1 and # for BEAS-2B cells); a and b $p < 0.05$ for comparing S- with M-SWCNTs (a is for THP-1 and b for BEAS-2B cells).

Author Manuscript Author Manuscript Author Manuscript Author Manuscript

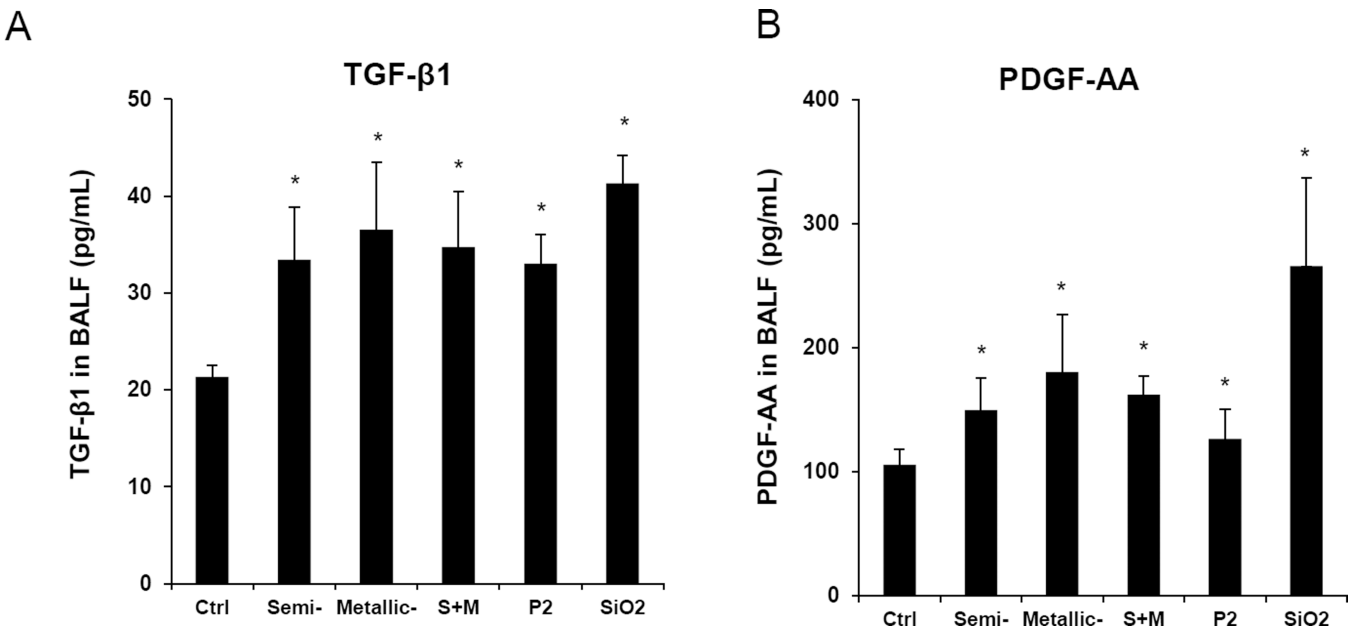

Author Manuscript Author Manuscript Author Manuscript Author Manuscript

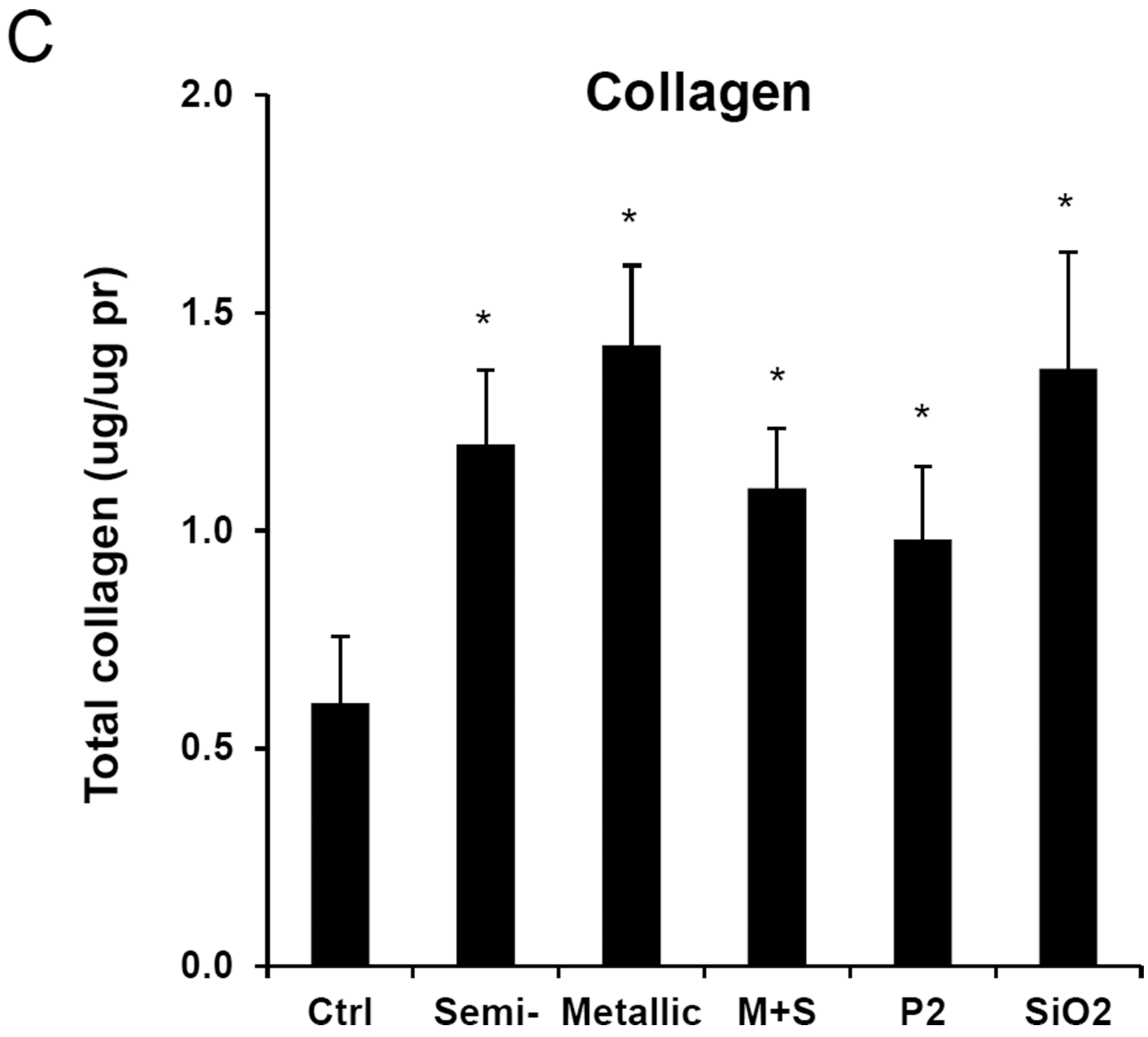

Author Manuscript Author Manuscript Author Manuscript Author Manuscript

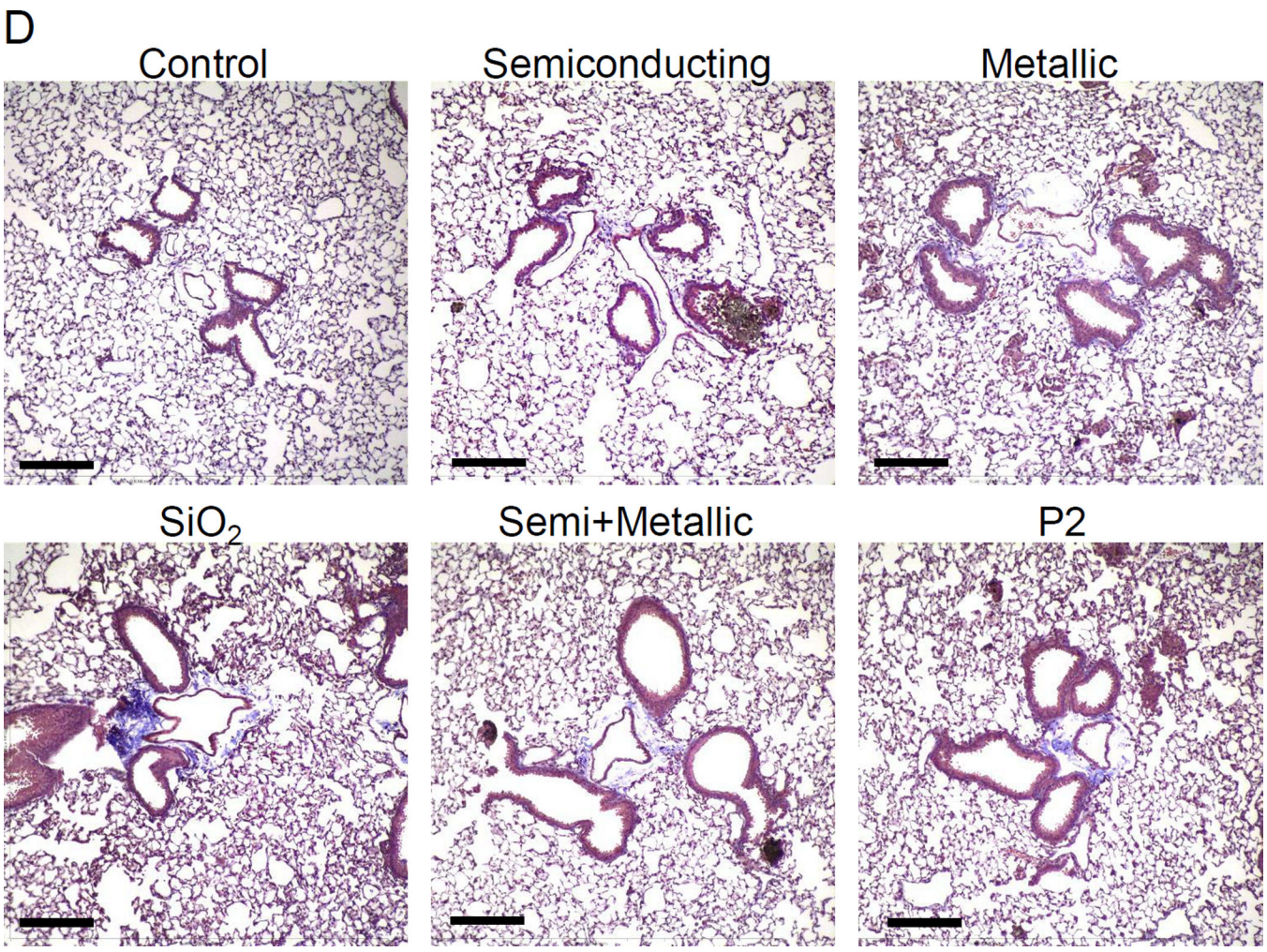

Figure 5. Assessment of the pro-fibrogenic effects of the electronic sorted SWNCTs in mice

Anesthetized C57BL/6 mice were exposed to SWNCTs, delivered by one-time oropharyngeal aspiration of a 2.0 mg/kg bolus dose. Animals were euthanized after 21 d, and BALF was collected to determine (A) TGF-β1 and (B) PDGF-AA levels. (C) Assessment of total collagen content by a Sircol kit (Biocolor Ltd., Carrickfergus, UK). *$p <$ 0.05 compared to control. (D) Visualization of collagen deposition in the lung, using Masson's trichrome staining. Collagen deposition is shown as blue staining under 100 × magnification. Animals exposed to Quartz (QTZ) served as positive control.

Author Manuscript Author Manuscript Author Manuscript Author Manuscript

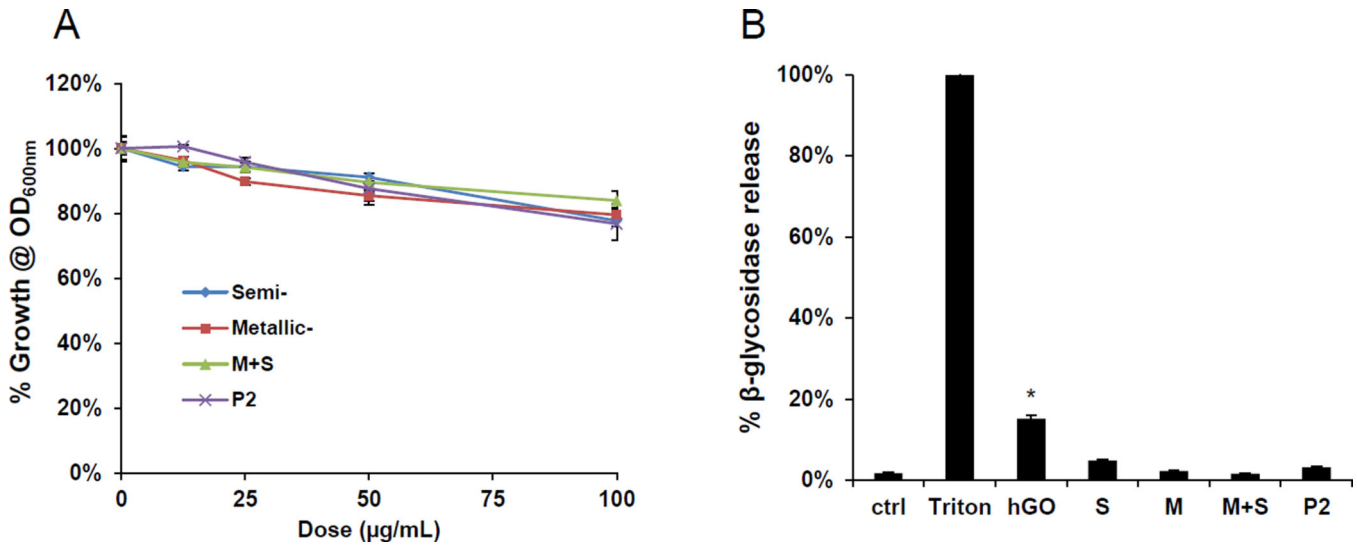

Author Manuscript Author Manuscript Author Manuscript Author Manuscript

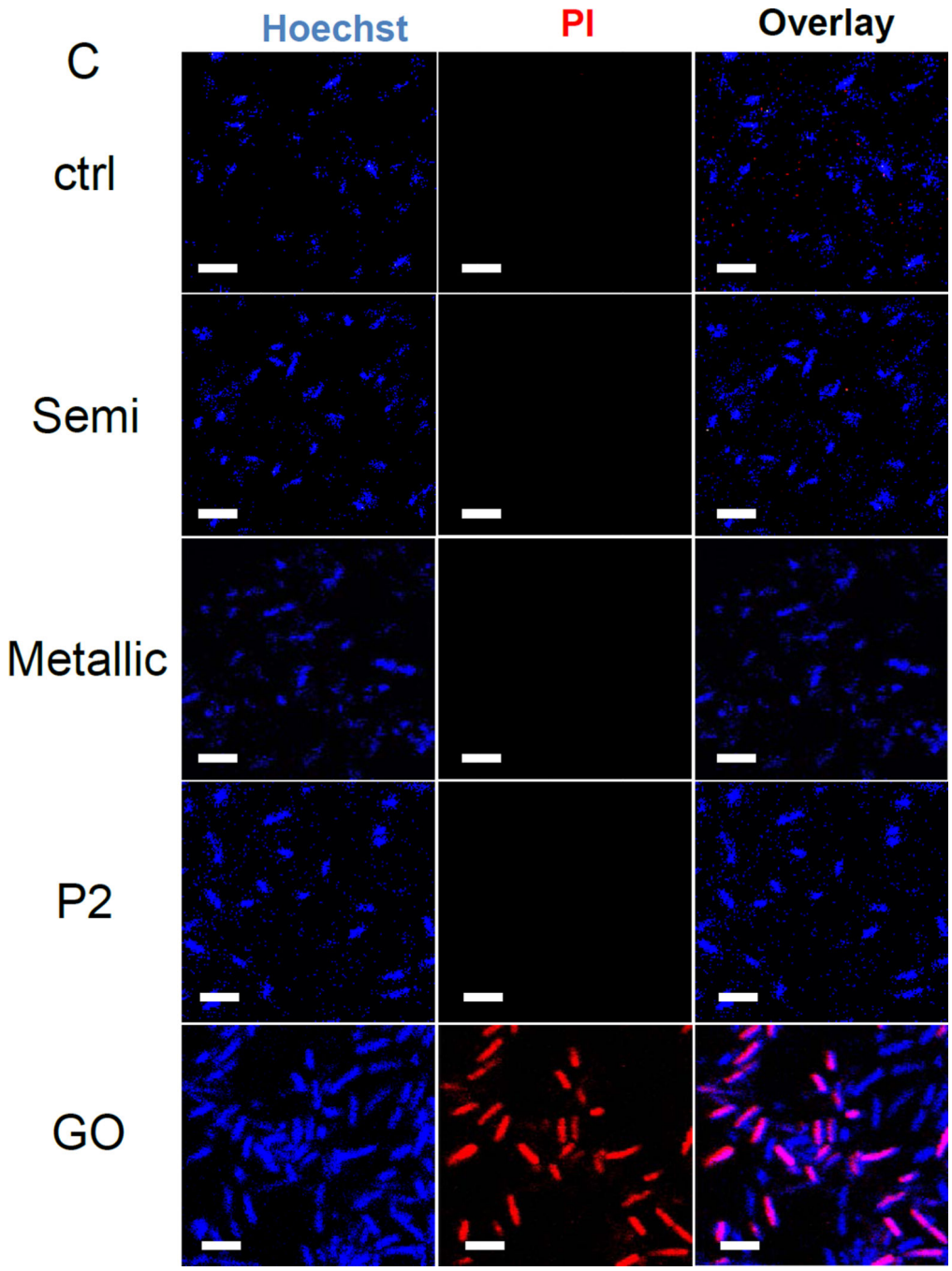

Author Manuscript Author Manuscript Author Manuscript Author Manuscript

D

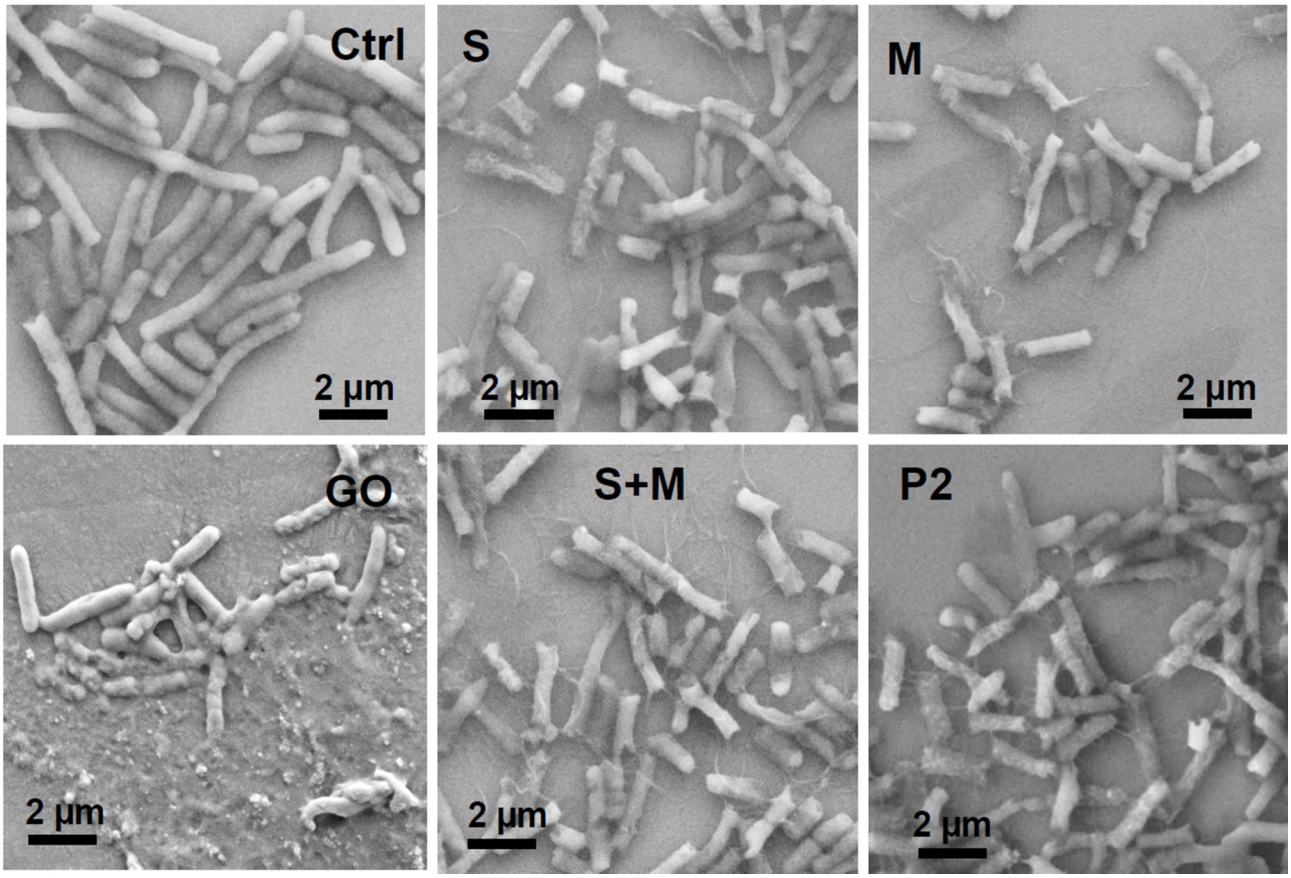

Figure 6. Assessment of the anti-bacterial effects of electronic-sorted SWNCTs in *E coli*

(A) Cellular growth was assessed in *E coli* using a Biotek Synergy plate reader (BioTek, Winooski, VT) at OD_{600}. The cultures were incubated with 12.5, 25, 50 and 100 μg/mL SWNCTs for 24 h. (B) Bacterial cell membrane integrity was evaluated by using a luminescent β-galactosidase substrate to measure the release of the enzyme into the culture supernatant during incubation with 100 μg/mL SWCNTs for 24 h. Triton X-100 membrane lysis was used as a positive control, and for comparative purposes, we also included graphene oxide (GO), which can permeabilize the cell membrane. * $p < 0.05$ compared to GO treatment. (C) Confocal microscopy to determine bacterial viability during PI staining. Bacteria were seeded into 8-well chamber slides and incubated with 100 μg/mL SWNCTs for 24 h, then the cells were stained with Hoechst 33342 (1 μM) and propidium iodide (5 μM) for 30 min. The cells were washed three times with PBS, and observed under a confocal 1P/FCS inverted microscope. GO was used as a positive control. The scale bars represent 2 μm in length. (D) Scanning electron microscopy (SEM) to determine the morphology change of *E. coli*. Bacteria grown on a glass substrate were exposed to the SWCNTs at 100 μg/mL for 24 h. After fixation and dehydration, the cells were imaged using a JEOL JSM-67 field emission scanning electron microscope at 10 kV.

Author Manuscript

Author Manuscript

Author Manuscript

Author Manuscript

Table 1

Hydrodynamic diameter and zeta potential of SWCNTs.

SWCNTs		In DI H_2O	In BEGM	In RPMI
Semi-	hydrodynamic size (nm)	1192 ± 94	1683 ± 68	1407 ± 99
	zeta potential (mV)	−34.3 ±1.7	− 8.8 ±1.0	−7.1 ± 0.4
Metallic-	hydrodynamic size (nm)	807 ± 229 nm	1369 ±161 nm	1107 ± 80 nm
	zeta potential (mV)	−12.9 ± 0.4	−6.9 ± 0.7	−4.3 ± 0.2
P2-	hydrodynamic size (nm)	880 ±175 nm	974 ± 14 nm	836 ± 23 nm
	zeta potential (mV)	−16.1 ± 0.1	−7.9 ± 0.5	−5.6 ± 0.1

The average length and diameter of the SWCNTs were assessed by UV-vis and TEM microscopy (JEOL 100 CX transmission electron microscope). The zeta potential was measured using a ZetaSizer Nano-ZS (Malvern Instruments, Worcestershire WR, U.K.). The hydrodynamic diameters in H_2O, BEGM, and RPMI were determined using high-throughput dynamic light scattering (HT-DLS, Dynapro Plate Reader, Wyatt Technology).